

Supporting Information

for

Magnetic Ordering in a Vanadium-Organic Coordination Polymer Using a Pyrrolo[2,3-*d*:5,4-*d'*]bis(thiazole)-based Ligand

Yulia A. Getmanenko,^{a} Christopher S. Mullins,^b Vladimir N. Nesterov,^c Stephanie Lake,^b*

Chad Risko^b and Ezekiel Johnston-Halperin^a

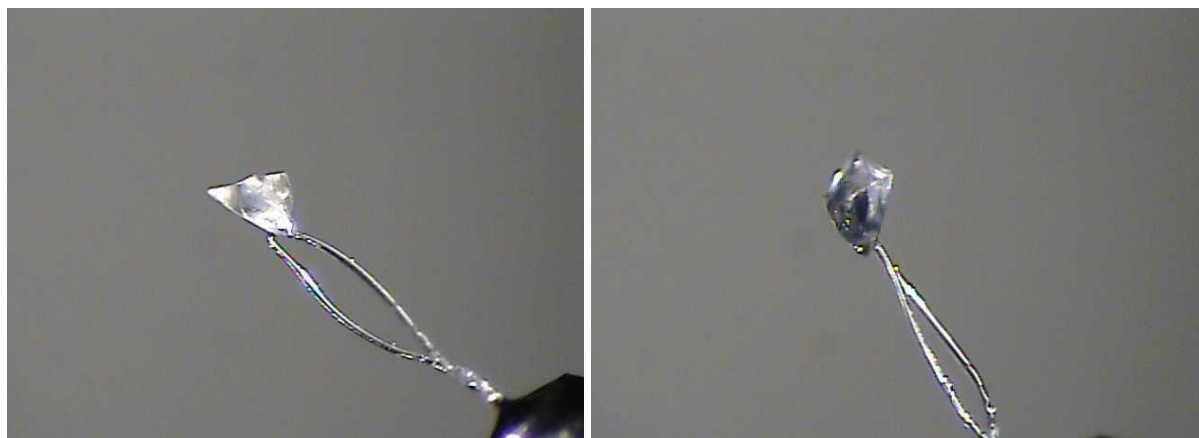


Figure S1. Photographs of single crystal of 4-hexyl-4*H*-pyrrolo[2,3-*d*:5,4-*d'*]bis(thiazole) (**5**).

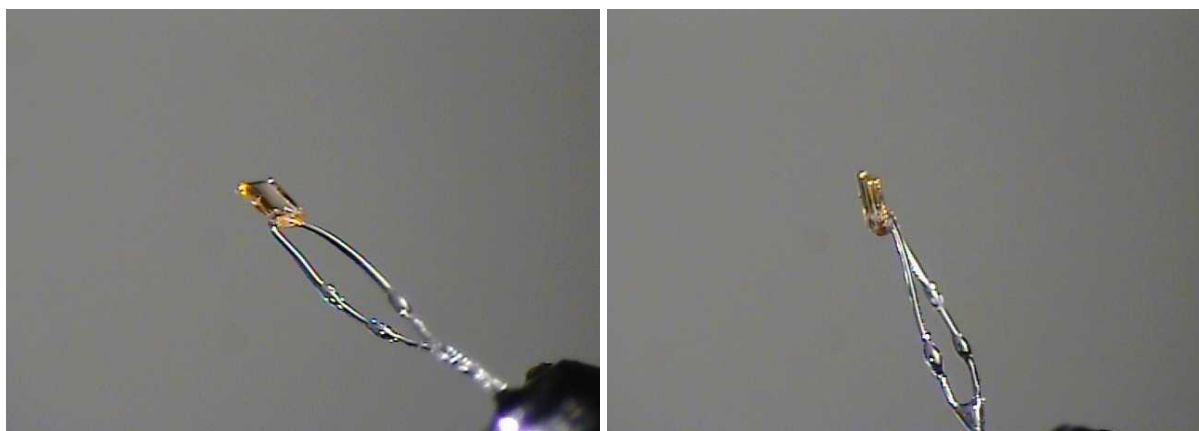


Figure S2. Photographs of a single crystal of 4-hexyl-2,6-diiodo-4*H*-pyrrolo[2,3-*d*:5,4-*d'*]bis(thiazole) (**6**)

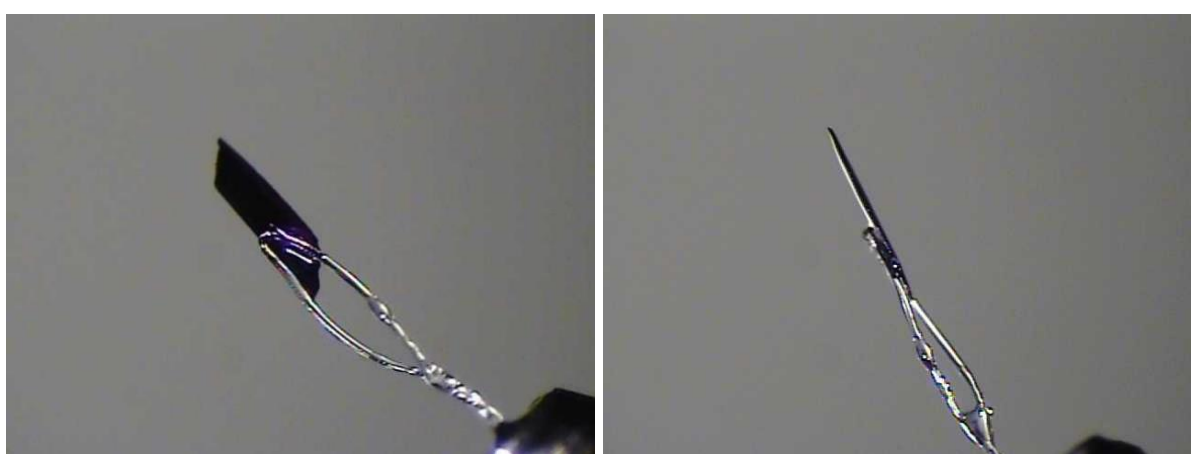


Figure S3. Photographs of a single crystal of ligand **7**.

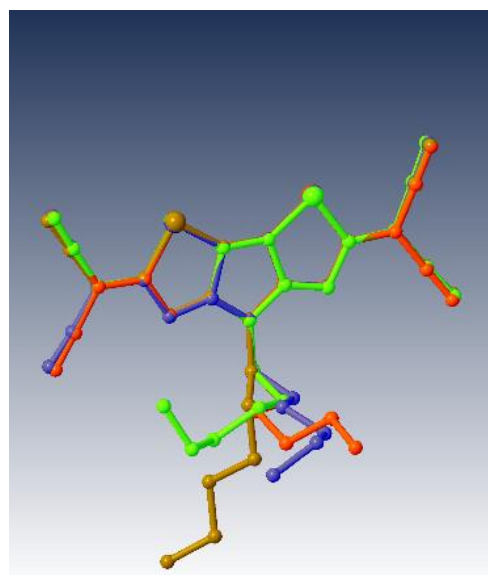


Figure S4. Overlay of the four independent molecules of compound **7** (1 is green; 1A is red; 1B is blue; 1C is brown).

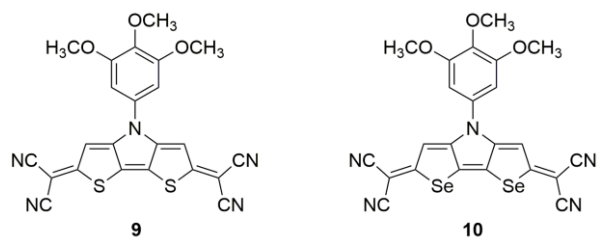


Figure S5. Structures of dithieno[3,2-*b*:2',3'-*d*]pyrrole (DTP) derivative (**9**) and diselenopheno[3,2-*b*:2',3'-*d*]pyrrole (DSP) derivative (**10**) investigated computationally.

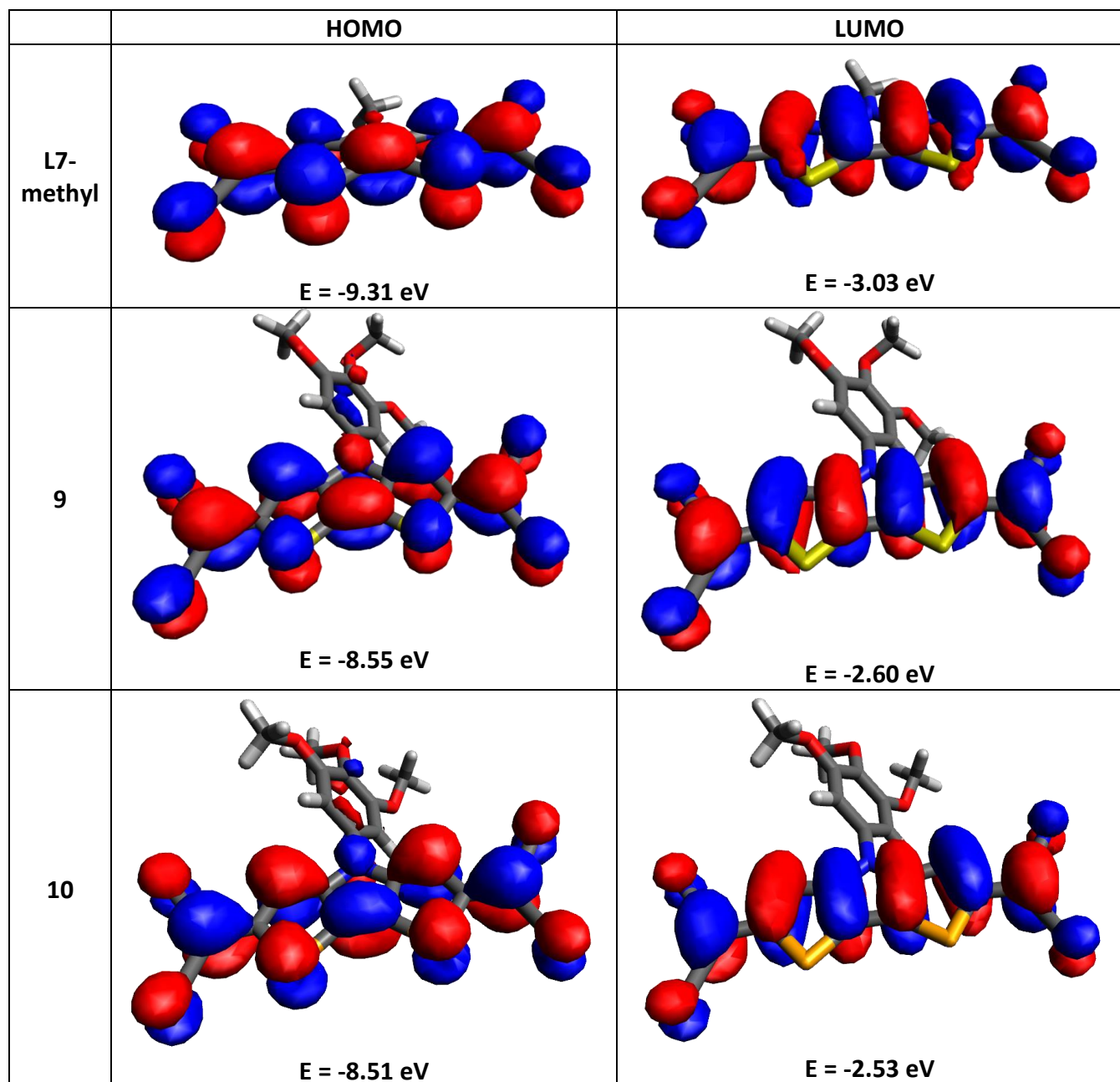
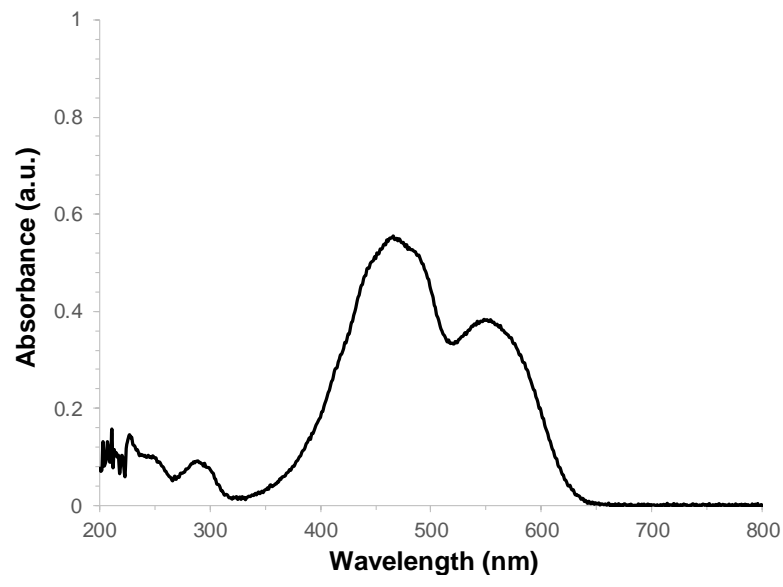
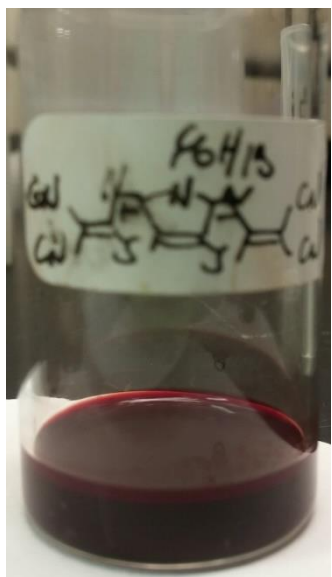


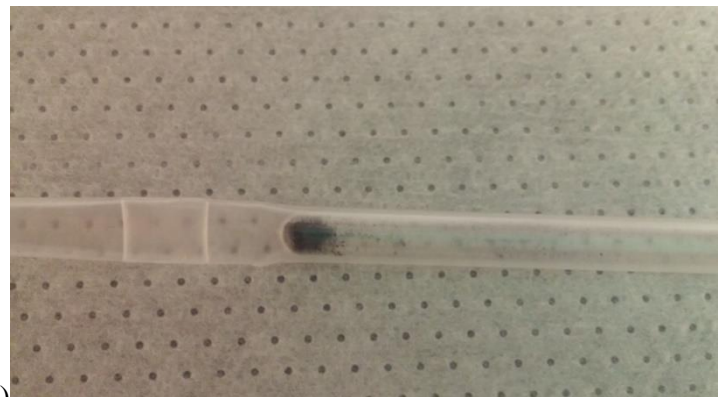
Figure S6. Pictorial representations and energies of the HOMO and LUMO for an *N*-methyl derivative of ligand **7** (**L7-methyl**), DTP derivative **9**, and DSP derivative **(10)** as determined at the OT-LC- ω PBE/cc-PVDZ level of theory.



(a)

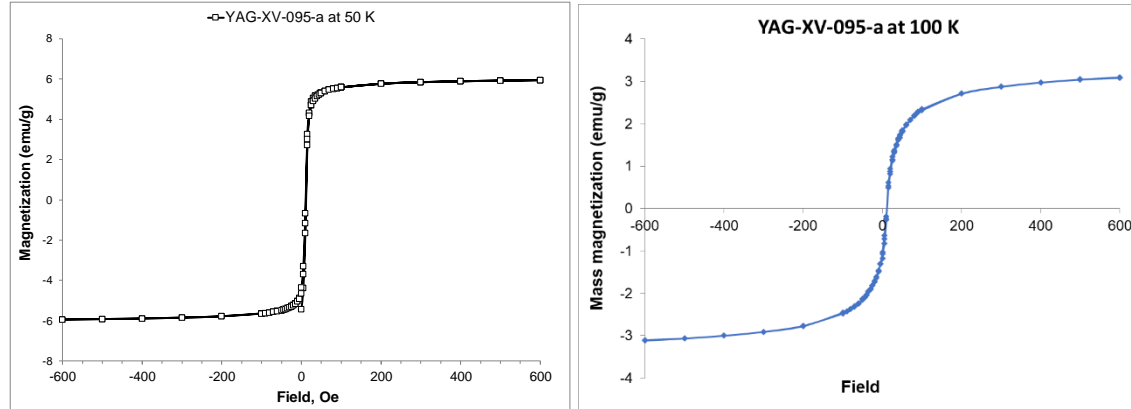
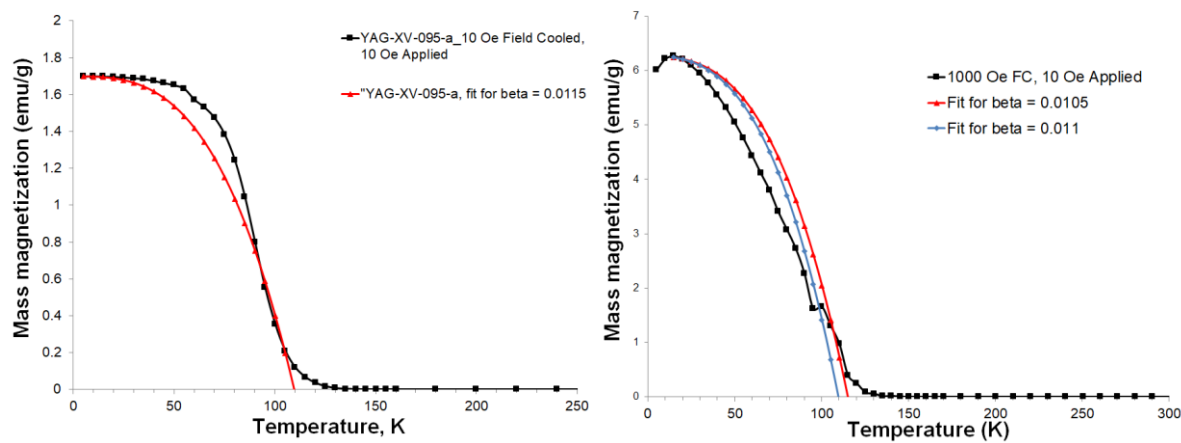


(b)



(c)

Figure S7.(a) UV-vis absorption spectra of ligand **7** in dichloromethane; (b) a photograph of a solution of ligand **7** in dichloromethane; (c) a photograph of the hybrid material **8** in a sealed quartz tube inside of a plastic straw.



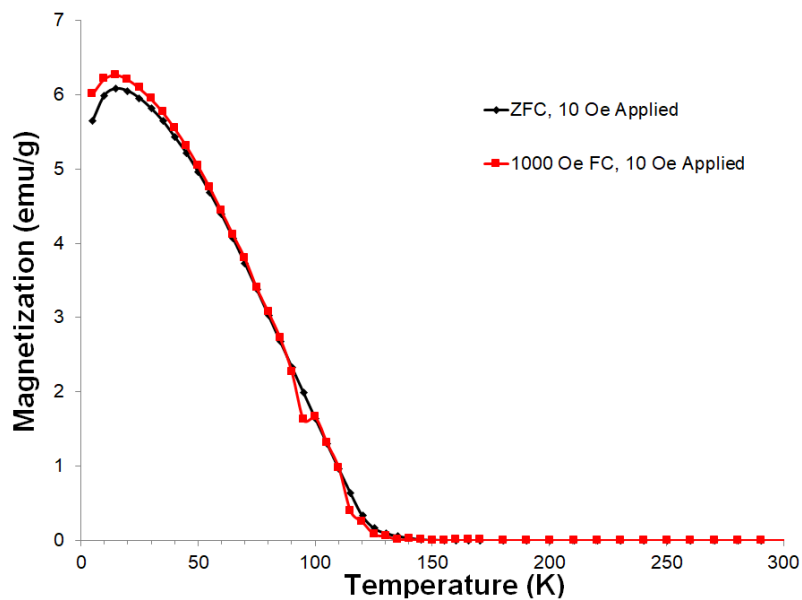


Figure S10. ZFC and FC temperature dependence of magnetization of material **8** (second independently prepared sample, YAG-XVI-022-b, ~1.1 mg of material **8** sealed in quartz tube).

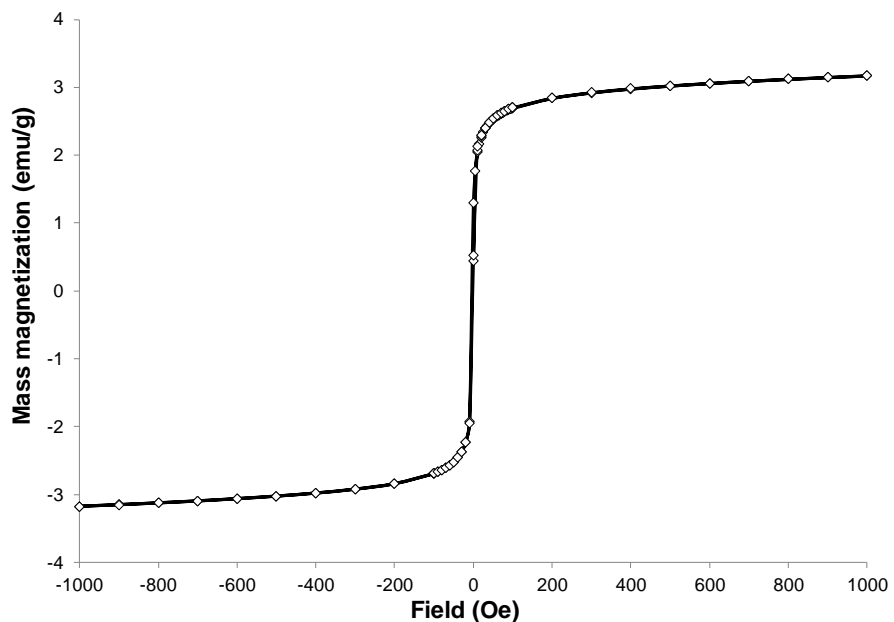


Figure S11. Hysteresis of **8** at 95 K (second independently prepared material, ~1.1 mg of YAG-XVI-022-b). Saturation magnetization is comparable to the 1st batch of **8** at 100 K (**Figure S9**, right).

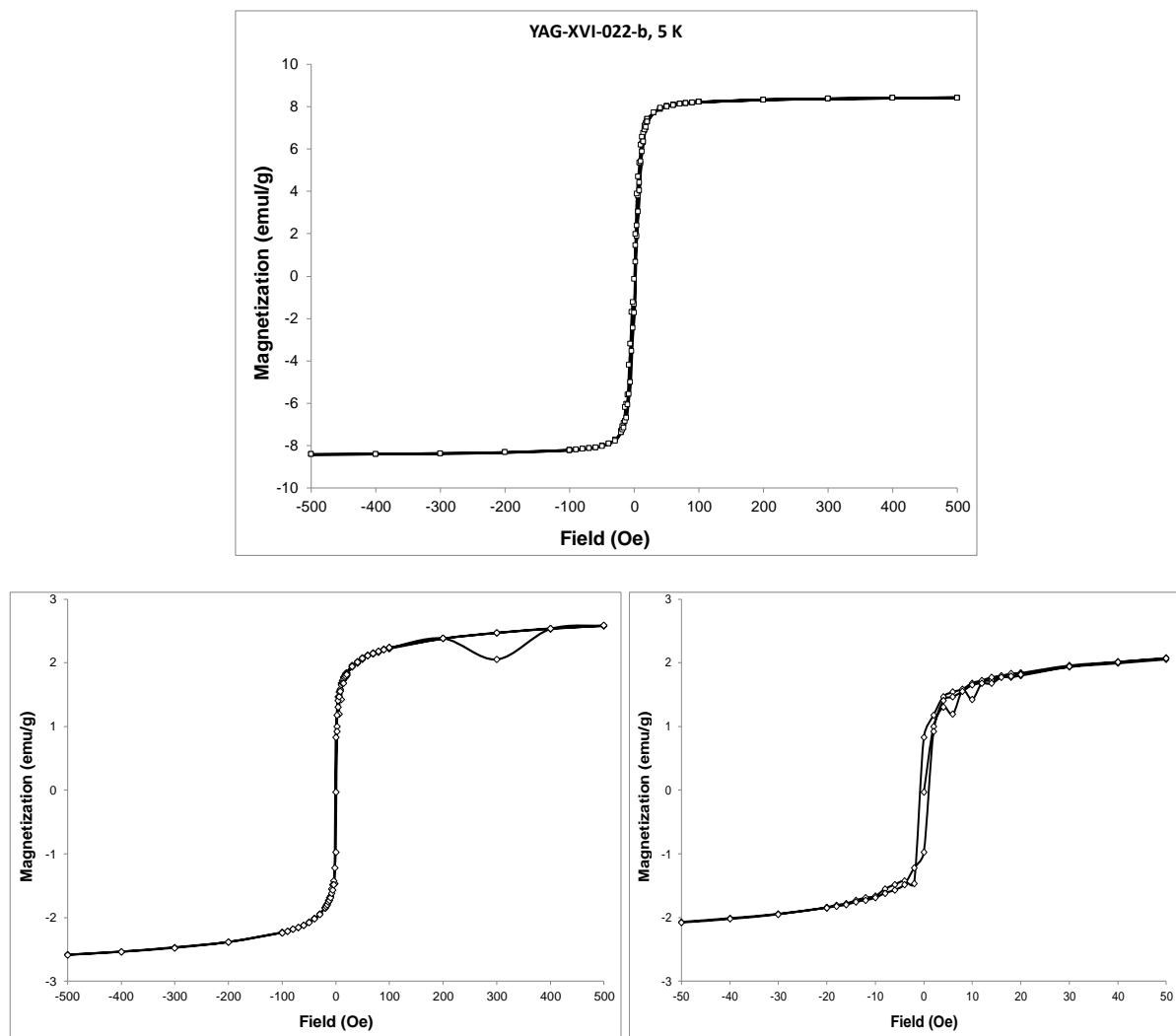


Figure S12. Hysteresis of material **8** (*top*) at 5 K, (*bottom left*) at 50 K and (*bottom right*) at 95 K for a second independently prepared sample (batch YAG-XVI-022-b). Saturation magnetization reached 8.4 emu·g⁻¹ at 500 Oe at 5 K (comparable to 7.8 emu·g⁻¹ measured for the first batch YAG-XIV-095-a).

Table S1. X-ray data and processing parameters for compounds **5-7**.

CCDC entry no.	1819816	1819817	1868490
Crystal system	Monoclinic	Monoclinic	Triclinic
Space group	<i>Cc</i>	<i>Cm</i>	P-1
a, Å	11.438(2)	16.8767(2)	15.8211(3)
b, Å	11.940(2)	33.8581(5)	15.8245(3)
c, Å	9.874(2)	4.4165(1)	16.6689(2)
α, deg	90	90	79.740(1)
β, deg	107.370(2)	91.650(1)	66.715(2)
γ, deg	90	90	73.107(2)
V, Å ³	1287.0(4)	2522.60(7)	3658.41(12)
Mol formula	C ₁₂ H ₁₅ N ₃ S ₂	C ₁₂ H ₁₃ I ₂ N ₃ S ₂	C ₁₈ H ₁₃ N ₇ S ₂
fw	265.39	517.17	391.47
Formula units per cell (Z)	4	6	8
D _{calcd} (Mg/m ³)	1.370	2.043	1.422
λ (Mo/Cu Kα), Å	0.71073	0.71073	1.54184
μ (mm ⁻¹)	0.395	3.979	2.794
Absorption correction	Semi-empirical from equivalents	Semi-empirical from equivalents	Semi-empirical from equivalents
Total reflections	6623	36525	48939
Independent reflections	2763	5624	14247
R _{int}	0.0183	0.0237	0.0754
Data/res/parameters	2763 / 2 / 156	5624 / 5 / 260	14247 / 0 / 977
R1 ^a [I ≥ 2σ(I)]	0.0203	0.0187	0.0468
wR2 ^b (all data)	0.0509	0.0479	0.1199
GOF on F ²	1.052	1.055	1.023
Δρ(max), Δρ(min) (e/Å ³)	0.141, -0.128	0.888, -0.681	0.583, -0.385

^aR1 = Σ||F_o| - |F_c||/Σ |F_o|; ^bR2 = {Σ[w(F_o² - F_c²)²]/Σ[w(F_o²)²]}^{1/2}

Table S2. Short intermolecular contacts between molecules of compound **7**.

Molecules 1···1A/1C	Distance Å	Molecules 1B/1A···1C/1B	Distance Å
S(1)···S(2A)	3.439(1)	S(1B)···S(2C)	3.500(1)
S(1)···N(6A)	2.974(2)	S(1B)···N(6C)	2.993(2)
S(2)···N(6A)	3.052(2)	S(2B)···N(6C)	3.091(2)
N(4)···S(1A)	3.070(2)	N(4B)···S(1C)	3.125(2)
N(4)···S(2A)	3.002(2)	S(2C)···N(4B)	3.056(2)
C(2)···N(7C)	3.006(2)	S(1A)···N(6B)	3.325(2)

Table S3. Comparison of the single-crystal X-ray structure for compound **7** and the OT-LC- ω PBE/cc-PVDZ optimized geometry for **L7-methyl**.

	Compound 7		L7-methyl
<u>Bond label</u>	<u>Distance (Å)</u>		<u>Distance (Å)</u>
C2-N2	1.369		1.371
C3-N2	1.378		1.371
C3-C5	1.467		1.461
C5-C6	1.352		1.359
C2-C6	1.463		1.462
N2-C13	1.473		1.450
C2-N1	1.300		1.295
N1-C1	1.378		1.365
C1-S1	1.786		1.801
S1-C6	1.712		1.729
C3-N3	1.294		1.295
N3-C4	1.381		1.365
C4-S2	1.776		1.801
S2-C5	1.720		1.729
<u>Angle label</u>	<u>Bond angle (°)</u>		<u>Bond angle (°)</u>
C1-S1-C6	88.21		87.90
C4-S2-C5	87.98		87.89
C1-N1-C2	107.23		108.66
C3-N3-C4	107.26		108.73

Table S4. Select information pertaining to the $S_0 \rightarrow S_1$ excitations as determined via TDDFT calculations at the OT-LC- ω PBE/cc-PVDZ level of theory.

Molecule	E [eV]	λ [nm]	f	Electronic Configuration	% contribution
L7-methyl	2.26	549	0.37	HOMO-1 \rightarrow LUMO; HOMO \rightarrow LUMO	43 56
TCNQ	3.13	396	1.08	HOMO \rightarrow LUMO	100
TCNE	4.80	258	0.43	HOMO \rightarrow LUMO	98
TCNB	4.62	268	0.04	HOMO-1 \rightarrow LUMO; HOMO \rightarrow LUMO+1	64 31
9	2.14	578	0.0036	HOMO-3 \rightarrow LUMO; HOMO-2 \rightarrow LUMO; HOMO-1 \rightarrow LUMO	37 7 54
	2.55	486	1.37	HOMO \rightarrow LUMO	100
10	2.00	618	0.0104	HOMO-3 \rightarrow LUMO; HOMO-2 \rightarrow LUMO; HOMO-1 \rightarrow LUMO	33 6 58
	2.53	491	1.30	HOMO \rightarrow LUMO	98